ASEG-PESA 2013
'THE EUREKA MOMENT'
11-14 AUGUST 2013 • MELBOURNE, AUSTRALIA

The inversion of data from complex 3-D resistivity and I.P. surveys

M.H.Loke
Geotomo Software
Penang, Malaysia.,
drmhloke@yahoo.com

K. Frankcombe
ExpolreGeo
Wangara, WA, Australia
kim@exploregeo.com.au

D.F.Rucker
Hydrogeophysics, Inc
Tucson, Arizona, USA
druck8240@gmail.com

SUMMARY

The search and recovery for base and precious metals in recent years has led to surveys in more challenging areas over complex deposits and in extreme terrains. Such deposits frequently have accessory minerals that can be detected by induced polarization (I.P.) surveys. Due to their complex shapes and host terrains, 3-D surveys and inversion models are necessary to accurately resolve them. However, in some cases, the survey lines are not arranged rectilinearly. To accommodate an arbitrary arrangement of the electrodes, a model discretisation that is independent of the electrode positions is used. The rugged terrain can be accurately modelled by the use of the finite-element method where the surface of the mesh matches the topography. Innovative arrays such as the offset pole-dipole array have been used to rapidly survey large areas at a lower cost compared to traditional dipole-dipole arrays. Such arrays frequently have large geometric factors that make it difficult to accurately calculate the I.P. anomalies with the conventional linear perturbation approach that uses the difference of two resistivity calculations. The complex resistivity method, where the I.P. component becomes the imaginary component of the resistivity model, avoids this problem as it effectively decouples the resistivity and I.P. calculations. Furthermore, time-lapse 3-D surveys using surface and borehole electrodes have been conducted to monitor the flow of sodium cyanide solution directly injected in steep-sided ore rock piles for secondary recovery of gold. A 4-D resistivity inversion method is used to map the flow of the solution during the injection process.

Key words: 3-D, resistivity, I.P., inversion, time-lapse

INTRODUCTION

The high price of base and precious metals in recent years has led to surveys in more challenging areas with complex geology and extreme terrains. Many mineral deposits have accessory minerals that can be detected by induced polarization (I.P.) surveys, which measures both resistive and capacitive aspects of the rock. Due to their complex shapes and host terrains, 3-D surveys and inversion models are necessary to accurately resolve them. The availability of practical 3-D inversion software for microcomputers have also made it possible to reinterpret data from old surveys for a more accurate re-appraisal of prospects. While modern 3-D field surveys attempt to arrange the electrodes in a rectilinear grid along parallel lines, old 2-D survey lines (particularly when acquired in multiple campaigns) frequently do not have a simple pattern.

The high price of gold has led to secondary recovery efforts by injecting sodium cyanide solution into ore rock piles. In order to optimise the secondary recovery process, it is necessary to monitor the flow of the solution during the injection process.

The following section describes different numerical methods that are used to produce more realistic models from 3-D surveys. This is followed by examples from two field surveys.

METHODS

This section briefly describes a few numerical techniques used to model the data from complex 3-D field surveys.

Smoothness-constrained least-squares inversion

The smoothness-constrained least-squares optimisation method is frequently used for 2-D and 3-D inversion of resistivity data (Loke et al., 2003). The subsurface model consists of a large number of cells so that any resistivity distribution can be accommodated. The equation that gives the relationship between the model parameters and the measured data is given below.

$$\left[\mathbf{J}_i^T\mathbf{R}_d\mathbf{J}_i + \lambda_i\mathbf{W}^T\mathbf{R}_m\mathbf{W}\right]\Delta\mathbf{r}_i = \mathbf{J}_i^T\mathbf{R}_d\mathbf{g}_i - \lambda_i\mathbf{W}^T\mathbf{R}_m\mathbf{W}\mathbf{r}_{i-1} \quad (1)$$

The Jacobian matrix **J** contains the sensitivities of the measurements with respect to the model parameters, $\boldsymbol{\lambda}$ is the damping factor vector and **g** is the data misfit vector. $\mathbf{r}_{i-1}$ is the model parameter vector (the logarithm of the model resistivity values) for the previous iteration, while is $\Delta\mathbf{r}_i$ is the change in the model parameters. **W** incorporates the roughness filters in the *x*, *y* and *z* directions. $\mathbf{R}_d$ and $\mathbf{R}_m$ are weighting matrices used so that different elements of the data misfit and model roughness vectors are given equal weights if the L1-norm inversion method is used (Loke et al., 2003).

Topography

Many mineral deposits occur in areas with extreme terrains that must be accurately modelled by the forward modelling routine used to calculate the model response. As the subsurface resistivity and I.P. can have arbitrary distributions, the finite-difference and finite-element methods are commonly used. Figure 1 shows the arrangement of mesh used by the two methods to model surface topography. As the finite-difference method normally uses a rectangular mesh, the surface topography is modelled by small rectangular steps (Figure 1a). The mesh cells above the ground are assigned a very high

resistivity value (eg. 10000 times the ground resistivity) to simulate the air layer. The finite-element method is more suitable as the position of the surface nodes can be adjusted to match the topography (Figure 1a) so that the topography is directly incorporated into the inversion model (Loke, 2000).

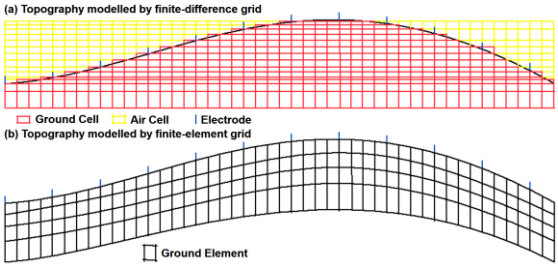

Figure 1. Topography modelling using the (a) finite-difference and (b) finite-element methods.

Large I.P. effects

There are two methods used to calculate I.P. effects, the perturbation (Oldenburg and Li, 1994) and the complex resistivity (Kenma *et al.*, 2000) methods. The first method assumes the intrinsic I.P. values are sufficiently small so that a linear perturbation of a base resistivity model can be used. Consider a base model that has a conductivity σ_{DC}. The effect of the chargeability m is to decrease the effective conductivity to $\sigma_{IP} = (1 - m)\ \sigma_{DC}$. The apparent I..P. ($m_a$) is then calculated by two forward models using the potentials (ϕ) from the original and perturbed conductivities.

$$m_a = [\ \phi(\sigma_{IP}) - \phi(\sigma_{DC})\ ] / \phi(\sigma_{DC}) \quad (2)$$

While perturbation approach works well in most cases, it has two main problems. Firstly it is based on the assumption that the intrinsic I.P. values are sufficiently 'small'. The second and more serious problem is that it's accuracy depends on the accuracy of two DC potentials. The difference is usually less than 1% of the potential values, so it magnifies numerical errors in the finite-difference or finite-element method used to calculate the DC potentials. For many arrays, this is usually not a problem. However, the offset pole-dipole and dipole-dipole arrays (White et al. 2001) can have very large geometric factors. In some situations, with large resistivity contrasts, this can sometimes lead to negative apparent resistivity values (Jung *et al.*, 2009). In such cases, the calculated apparent chargeability values are not reliable. The second I.P. model calculation method is to treat the conductivity as a complex quantity with real and imaginary components (Kenma *et al.*, 2000), which is given by

$$\sigma = \sigma_{DC} - i\, m\sigma_{DC}\,. \quad (3)$$

The DC conductivity σ_{DC} forms real part, while $m\sigma_{DC}$ forms the imaginary part. A complex potential, with two components ϕ_r and ϕ_i, is then calculated.

$$\phi = \phi_r + i\ \phi_i \quad (4)$$

The apparent chargeability is calculated using the ratio of the imaginary component to the real component, $m_a = \phi_i / \phi_r$. The accuracy of the apparent I.P. values does not depend on the accuracy of the D.C. potential.

Non-rectilinear survey grids

Modern 3-D surveys use an arrangement with the electrodes along a series of parallel lines. However, in areas with extreme topography, it might be necessary to deviate some of the lines. I.P. surveys along 2-D lines have been carried out since the 1950's. Interpretation of the data was mainly qualitative due to the lack of practical inversion software. In some areas, old data has been reinterpreted using modern software for a more accurate (and low cost) re-appraisal of old prospects. The surveys were rarely carried out along parallel lines, and frequently the lines have different directions. To interpret such data, it is necessary to use a flexible model discretisation that is not directly tied to the electrode positions (Figure 2). Each model block is subdivided by four mesh lines in the x and y directions (Figure 3). If the electrode falls on a node location (at the intersection of the mesh lines), it can be directly modelled by that node. There are two alternatives to model an electrode at a position when it does not fall on a mesh node. The first is by interpolating (Spitzer, 1999) the potentials (Figure 3a) at the four nearest nodes in the mesh (and similarly replace a current electrode by four equivalent current sources). The second method moves the nearest node to the location of the electrode using a distorted finite-element mesh (Figure 3b). This method can be used if the distance between two electrodes is more than the mesh spacing.

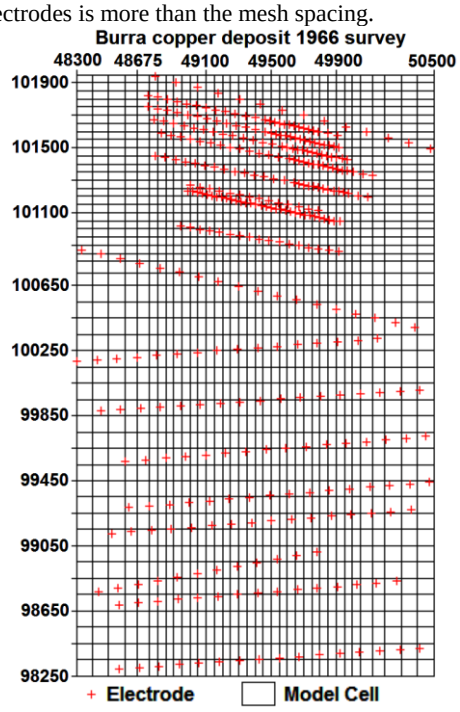

Figure 2. Example of surveys lines in different directions.

Time-lapse surveys

In some surveys, repeated 3-D measurements are carried out to detect temporal changes in the subsurface. The temporal changes in the resistivity are frequently much smaller than the spatial variations. Using the difference in models from independent inversions frequently display artefacts due to noise. To reduce the artefacts, a 4-D inversion methodology (Loke *et al.*, 2013) that directly incorporates the time domain with the space domain is used. The least-squares equation is modified to the following form.

$$\left[\mathbf{J}_i^T\mathbf{R}_d\mathbf{J}_i + \left(\lambda_i\mathbf{W}^T\mathbf{R}_m\mathbf{W} + \alpha\mathbf{M}^T\mathbf{R}_t\mathbf{M}\right)\right]\Delta\mathbf{r}_i = \mathbf{J}_i^T\mathbf{R}_d\mathbf{g}_i - \left(\lambda_i\mathbf{W}^T\mathbf{R}_m\mathbf{W} + \alpha_i\mathbf{M}^T\mathbf{R}_t\mathbf{M}\right)\mathbf{r}_{i-1} \quad (5)$$

M is the difference matrix applied across the time models with only the diagonal and one sub diagonal elements having values of 1 and -1, respectively. It minimises the difference in the resistivity of each model cell and the corresponding cell

for the next temporal model. α is the temporal damping factor that gives the relative weight for minimising the temporal changes in the resistivity compared to the model smoothness and data misfit.

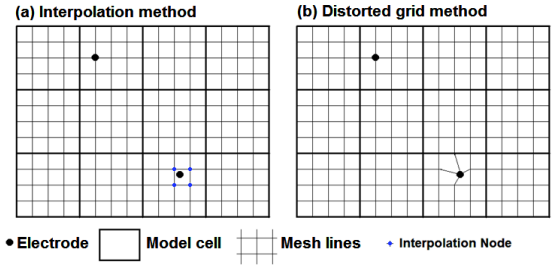

Figure 3. Methods to model the effect of an electrode not on a node using (a) interpolation and (b) distorted grid methods.

RESULTS

This section presents the results from two field surveys with complex geology and unusual field arrangements.

Burra, South Australia

The Burra copper deposit was discovered in 1845 and mining started in 1848 and ceased in 1877. It was at one time the largest copper mine in Australia. It was reopened in 1971 and closed again in 1981. Figure 2 shows some of the lines from a 1966 I.P. survey. Because of urban development and consequent restricted access for any new survey, a re-interpretation of the data was carried using modern 3-D inversion methods to glean more information from it. There is highly uneven data coverage. As such, the model use smaller 50x50 m. blocks in the northern part and larger 100x100 m. blocks towards the sides in the southern part. The inversion model shows a significant I.P. anomaly at the *x-y* location of about (49900,101400) at depths of between 100 to 200 m. (Figure 4b). At the same location, there is a region of generally lower resistivity values of about 40 to 90 ohm.m. This corresponds with the Eagle prospect, currently being drilled by Phoenix Copper, nearly 50 years after the survey! The north-south trending linear resistivity low, pfe high, coincides with the Kingston Fault and defines the line of lode in the Burra field. The nature of the high I.P. anomalies towards the bottom-left edge of the deeper layers is uncertain as there is not much data coverage there. They enticingly lie on interpreted structures with the eastern most anomaly lying in the Kingston Fault, but neither have been tested. Figure 5 shows the resistivity and I.P. models as 3-D plots.

Cripple Creek, Colorado

Sodium cyanide solution was injected into ore rock piles for secondary recovery of gold after surface leaching had ceased at the Cripple Creek and Victor Gold Mine in Colorado, USA in September 2011. Resistivity measurements were made to monitor the flow of the solution so as to optimise gold recovery. The measurements were made using 48 electrodes on the ground surface arranged in a radial pattern (Figure 6), 94 electrodes along six boreholes and 8 long electrodes using steel-case injection wells (Rucker *et al.*, 2013). Each snapshot took 14 minutes to complete, and a total of 780 snapshots were acquired. The positions of the electrodes together with the surface topography are shown in Figure 6b. Due to the use of a radial layout, the data coverage is very sparse towards the edges of the model grid (Figure 6a). As resistivity distribution within the ore heaps is highly inhomogeneous, the change in the resistivity is used to monitor the flow of the solution. Figures 6b and 6c shows the results from one series of measurements in the form of iso-surface contours for the -4% change in the resistivity at different times. Note the area with the largest change is located to the north of the well. This is probably due to differences in the subsurface permeability and structural nonuniformities within the heap created during end-dump construction (Rucker *et al.*, 2013). The heap was built up over the past 20 years by trucks dumping fresh ore over the edge of older ore.

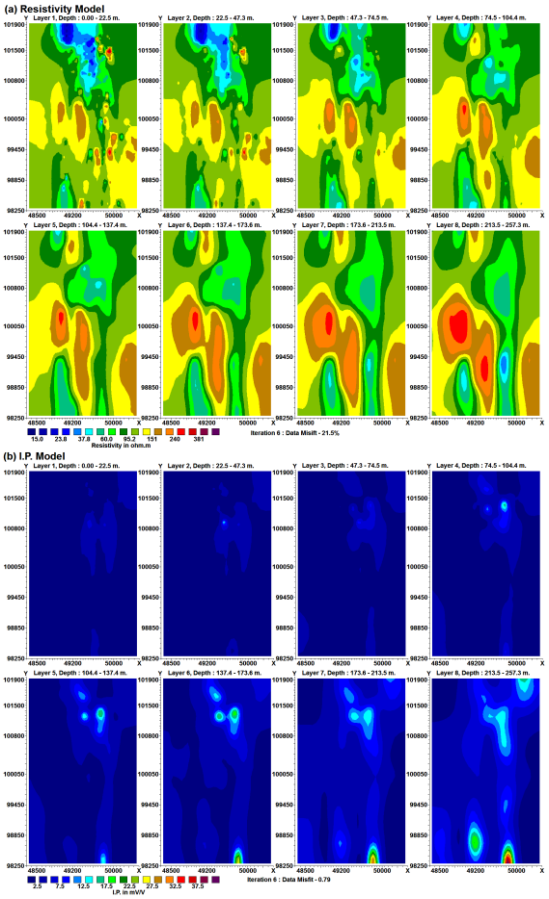

Figure 4. Resistivity and I.P. models for the Burra survey shown in the form of layers. The depths given are distances from the ground surface.

CONCLUSIONS

The search for mineral resources in increasingly more challenging environments using 3-D I.P. surveys require parallel improvements in data interpretation techniques to provide more realistic subsurface models. The use of the smoothness-constrained least-squares inversion method, and the finite-element method for areas with topography, enable the use of sufficiently fine model discretisations that can match the complex geology. The use of the complex resistivity method to calculate I.P. effects avoids the problem of numerical errors in the forward modelling routine when arrays with large geometric factors are used. A 4-D time-lapse inversion methodology using smoothness constraints in both

the spatial and temporal domains enables the accurate mapping of temporal changes.

ACKNOWLEDGMENTS

We would like to thank AngloGoldAshanti for the permission to use Cripple Creek data set, and Phoenix Copper for the Burra data set.

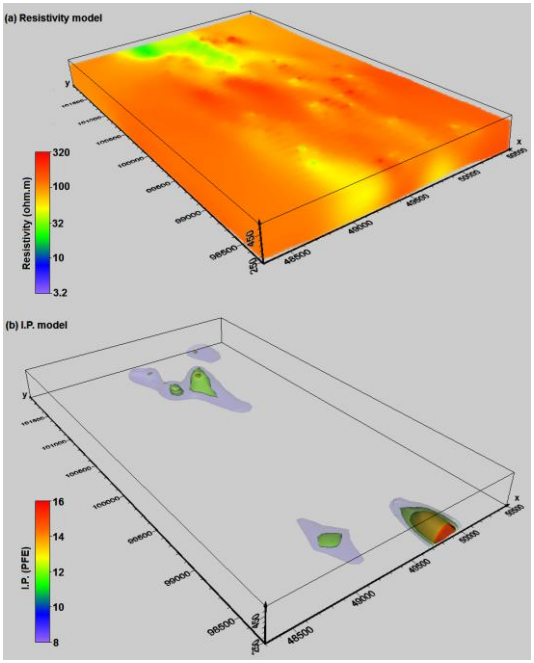

Figure 5. 3-D views of the Burra model showing (a) resistivity as rendered volume, (b) I.P. as isosurfaces with 9, 12 and 15 % PFE.

REFERENCES

Jung, H.K., Min, D.J., Lee, H.S., Oh, S.H., and Chung, H., 2009, Negative apparent resistivity in dipole–dipole electrical surveys: Exploration Geophysics 40, 33–40.

Kenma, A., Binley, A., Ramirez, A. and Daily, W., 2000. Complex resistivity tomography for environmental applications. Chemical Engineering Journal, 77, 11-18.

Loke, M.H., 2000, Topographic modelling in resistivity imaging inversion: 62nd EAGE Conference & Technical Exhibition Extended Abstracts, D-2.

Loke, M.H., Acworth, I., Dahlin, T., 2003, A comparison of smooth and blocky inversion methods in 2D electrical imaging surveys: Exploration Geophysics 34 , 182-187.

Loke, M.H., Dahlin, T. and Rucker, D.F., 2013, Smoothness-constrained time-lapse inversion of data from 3-D resistivity surveys. Near Surface Geophysics (in press).

Oldenburg, D. W., and Li, Y., 1994, Inversion of induced polarization data: Geophysics 59, 1327-1341.

Rucker, D.F., Crook N., Winterton J., McNeill M., Baldyga C.A., Noonan G. and Fink, J.B., 2013, Real-Time Electrical Monitoring of Reagent Delivery during a Subsurface Amendment Experiment. Near Surface Geophysics (in press).

Spitzer K., Chouteau M. and Boulanger O. 1999, Grid-independent electrode positioning for 3D DC and IP forward modeling: Proc. 2nd. Internat. Sym. 3D Electromagnetics, 189–192.

White, R.M.S., Collins, S., Denne, R., Hee, R., Brown, P., 2001, A new survey design for 3D IP modelling at Copper Hill: Exploration Geophysics 32, 152-155.

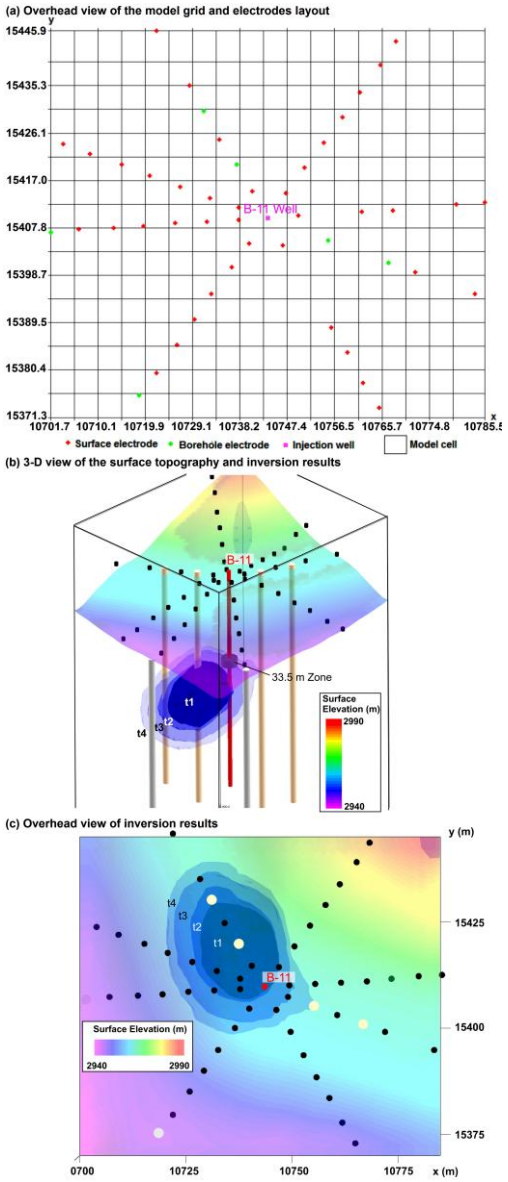

Figure 6. Cripple Creek survey. (a) Overhead view of the inversion model grid with electrodes layout. (b) Iso-surface contours for the -4% resistivity change at different times after the injection of the sodium cyanide solution (that started at 2.8 hours from the first data set in snapshots used). t1= 1.1 hours, t2= 2.4 hours, t3= 3.7 hours, t4= 4.9 hours. (c) Overhead view of iso-surfaces.